Research Article

Yaowalak Srisuwan, Prasong Srihanam, Theeraphol Phromsopha, and Yodthong Baimark*

Effect of citric acid on thermal, phase morphological, and mechanical properties of poly(L-lactide)-*b*-poly(ethylene glycol)-*b*-poly(L-lactide)/thermoplastic starch blends

https://doi.org/10.1515/epoly-2023-0057
received May 27, 2023; accepted September 09, 2023

Abstract: This work investigated the thermal, morphological, and tensile properties of poly(L-lactide)-*b*-poly(ethylene glycol)-*b*-poly(L-lactide) (PLLA-PEG-PLLA)/thermoplastic starch (TPS) blends with 3 wt% citric acid (CA) treatment of TPS. The blends with PLLA-PEG-PLLA/CA-TPS ratios of 100/0, 90/10, 80/20, and 60/40 (w/w) were investigated and compared with PLLA-PEG-PLLA/CA-free TPS blends. Crystallizability of the blends decreased and thermal stability increased as the TPS content increased. The thermal stability of the blends was found to improve after CA treatment of TPS. The PLLA-PEG-PLLA/CA-TPS blends showed better phase compatibility than those of the PLLA-PEG-PLLA/CA-free TPS blends. The tensile properties of the blends were improved by CA treatment of TPS. In conclusion, improvement in thermal stability, phase compatibility, and tensile properties of the PLLA-PEG-PLLA/TPS blends was obtained by CA treatment of TPS. The resulting PLLA-PEG-PLLA/CA-TPS blends could potentially be used to prepare biodegradable and flexible bioplastics.

Keywords: polylactide, block copolymer, thermoplastic starch, citric acid, phase compatibility

*** Corresponding author: Yodthong Baimark**, Biodegradable Polymers Research Unit, Department of Chemistry and Centre of Excellence for Innovation in Chemistry, Faculty of Science, Mahasarakham University, Mahasarakham 44150, Thailand, e-mail: yodthong.b@msu.ac.th
Yaowalak Srisuwan: Biodegradable Polymers Research Unit, Department of Chemistry and Centre of Excellence for Innovation in Chemistry, Faculty of Science, Mahasarakham University, Mahasarakham 44150, Thailand
Prasong Srihanam, Theeraphol Phromsopha: Biodegradable Polymers Research Unit, Department of Chemistry and Centre of Excellence for Innovation in Chemistry, Faculty of Science, Mahasarakham University, Mahasarakham 44150, Thailand

1 Introduction

An important synthetic bioplastic is poly(L-lactic acid) or poly(L-lactide) (PLLA) because of its bio-renewability, biocompatibility, and biodegradability (1–6). The utilization of PLLA in plastic applications is considered to solve the problem of non-biodegradable petroleum-based plastic waste (7). However, low flexibility and high production cost of PLLA are the main drawbacks compared with traditional petroleum-based plastics which restrict its range of applications (8–12).

Poly(L-lactide)-*b*-poly(ethylene glycol)-*b*-poly(L-lactide) (PLLA-PEG-PLLA) block copolymers are more flexible and more hydrophilic than PLLA due to the characteristics of PEG blocks (13–15). PLLA-PEG-PLLA reacts with a chain extender by post melt blending (14,15) and by *in situ* ring-opening polymerization (16) to control its melt flow ability for conventional melt processing. PLLA-PEG-PLLA is blended with low-cost thermoplastic starch (TPS) to reduce its production cost and to increase its biodegradation rate (17,18). The results showed that the PLLA-PEG-PLLA/TPS blends exhibited good phase compatibility compared with the PLLA/TPS blends. However, blending of TPS decreased the flexibility of PLLA-PEG-PLLA due to poor mechanical properties of TPS (12,19,20). Thus, the improvement in flexibility of PLLA-PEG-PLLA/TPS blends emerged as a challenge in this work.

Wang et al. (21,22) prepared PLLA/cornstarch blends in the presence of glycerol and citric acid (CA) by one-step extrusion processing. They found that the starch was degraded by CA treatment to improve the dispersion and compatibility in the blends. Kahar et al. (23) systematically investigated the effect of CA on the blend morphology and tensile properties of polyethylene/natural rubber/TPS blends. They found that the phase compatibility improved and the tensile properties increased after CA modification of TPS. Ibrahim et al. (24) treated TPS with CA to improve compatibility in PLLA/TPS blends. The results demonstrated that

tensile stress, strain at break, and Young's modulus of the PLLA/TPS blends increased when the TPS was treated with CA. The tensile stress and Young's modulus of the blends increased with the CA content until CA content was 3 wt%. However, PLLA-PEG-PLLA/TPS treated with CA blends have not been reported so far. Thus, we hypothesized that CA treatment of TPS could improve phase compatibility and tensile properties of the PLLA-PEG-PLLA/TPS blends.

The objective of this work was to improve phase compatibility and tensile properties of the PLLA-PEG-PLLA/TPS blends by CA treatment. For this purpose, TPS was treated with CA before melt blending with PLLA-PEG-PLLA. The effects of CA treatment and blend ratio on the thermal, morphological, and tensile properties of the PLLA-PEG-PLLA/TPS blends were determined and discussed. The PLLA-PEG-PLLA/CA-free TPS blends were also prepared for comparison.

2 Materials and methods

2.1 Materials

A chain-extended PLLA-PEG-PLLA with melt flow index of 26 g·10 min^{-1} (determined at 190°C under 2.16 kg load force) was synthesized in our research unit, as described in our previous work (16). TPS, (Tapioplast^{TM}) prepared from tapioca starch (79% amylopectin) was supplied by SMS Corporation Co., Ltd. (Pathum Thani, Thailand). CA was obtained from Merck.

2.2 CA treatment of TPS

TPS and CA were dried at 50°C under vacuum overnight before melt blending using a HAAKE PolyLab OS Rheomix batch-mixer (Thermo Scientific, USA) at 150°C for 10 min with a rotor speed of 100 rpm. TPS with and without 3 wt% CA treatment was prepared and designed as 3% CA-TPS and CA-free TPS, respectively.

2.3 Preparation of PLLA-PEG-PLLA/TPS blends

PLLA-PEG-PLLA and 3% CA-TPS were dried at 50°C under vacuum overnight before melt blending in a HAAKE PolyLab OS Rheomix batch-mixer (Thermo Scientific, USA) at 180°C for 5 min with a rotor speed of 100 rpm. PLLA-PEG-PLLA/3% CA-TPS blends with blend ratios of 100/0, 90/10, 80/20, and 60/40 (w/w) were investigated. PLLA-PEG-PLLA/CA-free TPS blends were also prepared by the same method for comparison.

2.4 Characterization of treated TPS and PLLA-PEG-PLLA/TPS blends

The reaction between TPS and CA was characterized with a Fourier-transform infrared (FTIR) spectrometer (Invenio-S, Bruker) equipped with an attenuated total reflectance accessory in the range of 4,000−500 cm^{-1} with a 4 cm^{-1} resolution and 32 accumulated scans.

The thermal transition properties of the blends were determined with a Pyris Diamond differential scanning calorimeter (DSC, Perkin Elmer) over the temperature range 0–200°C with a heating rate of 10°C·min^{-1} under a nitrogen gas flow. Thermal history of the blends was erased by melting at 200°C for 3 min followed with fast quenching to 0°C with cooling rate of 100°C·min^{-1} before the DSC heating scan. The degree of crystallinity (X_c) of the blend was calculated using Eq. 1 (9). Each DSC result was the average from three measurements.

$$X_c(\%) = [(DH_m - DH_{cc})/(93.6´W_{PLLA})] \times 100 \quad (1)$$

where ΔH_m and ΔH_{cc} are enthalpies of melting and cold crystallization, respectively. The ΔH_m of 100% X_c PLLA is 93.6 J·g^{-1} (9,25). W_{PLLA} is the PLLA weight fraction.

The thermal decomposition properties of the blends were determined with a SDT Q600 thermogravimetric analyzer (TGA, TA-Instrument) over the temperature range of 50–1,000°C at a heating rate of 20°C·min^{-1} under a nitrogen gas flow.

The phase morphology of cryofractured surfaces for the blend films were examined with a JSM-6460LV scanning electron microscope (SEM, JEOL) at an acceleration potential of 15 kV. Cryofracture surfaces were prepared by fracturing under liquid nitrogen. The samples were sputter-coated with gold prior to scan.

The tensile properties of the blend films (100 mm × 10 mm) were measured with a LY-1066B universal mechanical tester (Dongguan Liyi Environmental Technology Co., Ltd) at 25°C with a 100 kg load cell, a 50 mm·min^{-1} crosshead speed, and a 50 mm gauge length. Each tensile property was averaged from at least five samples.

3 Results and discussion

3.1 FTIR analysis

The FTIR spectra of the CA-free TPS and 3% CA-TPS are shown in Figure 1. They showed broad peaks in the range

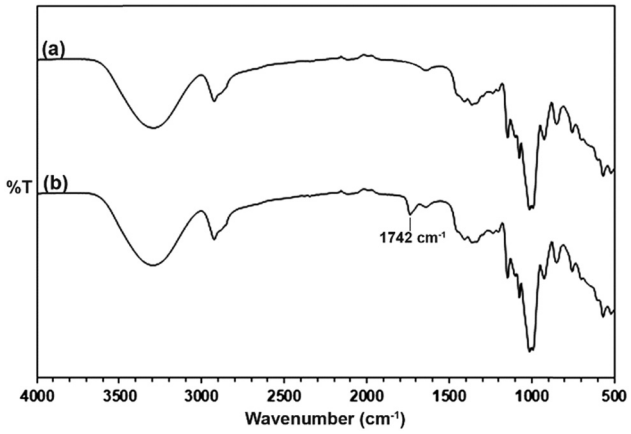

Figure 1: FTIR spectra of (a) CA-free TPS and (b) 3% CA-TPS.

of 3,700–3,000 cm^{-1} referred to the stretching hydroxyl groups, the peaks at 2,925 cm^{-1} attributed to the C–H stretching groups, and the peaks at 1,640 cm^{-1} related to the bending hydroxyl groups of starch (17,18,26). For 3% CA-TPS in Figure 1(b), an additional peak at 1,742 cm^{-1} assigned to the ester carbonyl groups of the TPS treated with CA was detected (23,27). This confirmed that an acetylation reaction between the hydroxyl groups of starch and carboxylic acid groups of CA had occurred (23,24).

Figure 2 shows expanded FTIR spectra of TPS in the region of C–O stretching vibration. The peaks at 1,150 cm^{-1} referred to C–O stretching vibration of C–O–H groups of starch (23). The height of this peak for 3% CA-TPS in Figure 2 (red line) was higher than that of the CA-free TPS in Figure 2 (black line) using the peak at 758 cm^{-1} (C–O–C ring vibration in starch) as the reference peak. This indicates the content of C–O–H groups of 3% CA-TPS was more than the CA-free TPS. The results implied that glycosidic

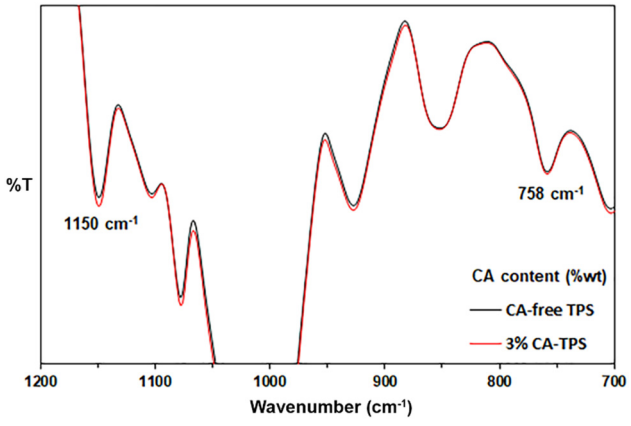

Figure 2: Expanded FTIR spectra in C–O stretching region (700–1,200 cm^{-1}) of CA-free TPS and 3% CA-TPS.

bonds of starch were hydrolyzed with CA to form new hydroxyl groups (23). The molar mass of starch then decreased by acid-catalyzed hydrolysis with CA (28).

3.2 Thermal transition properties

The thermal transition properties of the blends with and without 3% CA treatment including glass transition temperature (T_g), cold crystallization temperature (T_{cc}), melting temperature (T_m), and degree of crystallinity (X_c) were investigated from DSC heating curves as shown in Figure 3. The DSC results are summarized in Table 1. All the blends had similar T_g values in the range of 30–33°C. The T_{cc} and T_m values of pure PLLA-PEG-PLLA were 71.3°C and 159.6°C, respectively. The T_{cc} peaks shifted to higher temperatures (73.8–78.0°C) and the T_m peaks shifted to lower temperatures (156.4–157.8°C) when the TPS was incorporated. This shifting of T_{cc} and T_m peaks suggested that the cold crystallization of PLLA end-blocks was suppressed by the addition

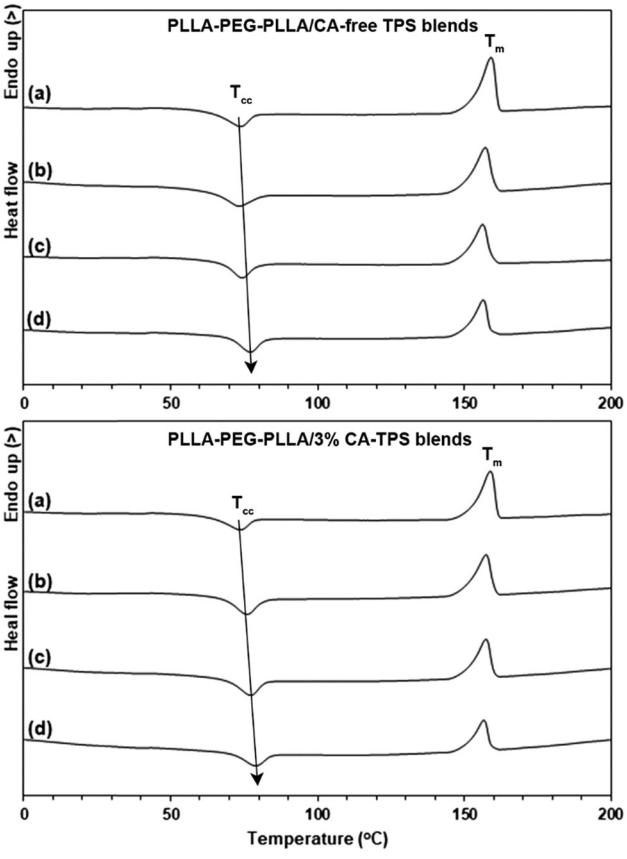

Figure 3: DSC heating curves of (top) PLLA-PEG-PLLA/CA-free TPS and (bottom) PLLA-PEG-PLLA/3% CA-TPS blends for blend ratios of (a) 100/0, (b) 90/10, (c) 80/20, and (d) 60/40 (w/w).

Table 1: Thermal transition properties of PLLA-PEG-PLLA/TPS blends with and without CA treatment

PLLA-PEG-PLLA/TPS (w/w)	T_g (°C)	T_{cc} (°C)	T_m (°C)	X_c (%)
Pure PLLA-PEG-PLLA	30.0 ± 0.6	71.3 ± 0.3	159.6 ± 0.2	25.2 ± 0.4
PLLA-PEG-PLLA/CA-free TPS				
90/10	31.4 ± 0.2	73.8 ± 0.2	157.3 ± 0.1	22.4 ± 0.5
80/20	32.2 ± 0.2	74.1 ± 0.3	156.6 ± 0.2	19.8 ± 0.4
60/40	33.0 ± 0.3	76.4 ± 0.1	156.4 ± 0.3	17.6 ± 0.7
PLLA-PEG-PLLA/3% CA-TPS				
90/10	32.5 ± 0.4	76.2 ± 0.2	157.8 ± 0.4	19.4 ± 0.6
80/20	32.3 ± 0.2	77.3 ± 0.3	157.3 ± 0.2	18.2 ± 0.5
60/40	30.4 ± 0.7	78.0 ± 0.1	157.4 ± 0.1	13.9 ± 0.4

of TPS and induced formation of imperfect PLLA crystallites (17). The T_{cc} peaks slightly shifted to higher temperature as the TPS content increased. However, the TPS content did not significantly affect shifting of the T_m peaks.

All the blends had X_c values (13.9–22.4%) lower than the pure PLLA-PEG-PLLA (25.2%). The X_c values steadily decreased as the TPS content increased for both the blend series. It should be noted that the X_c values of the PLLA-PEG-PLLA/3% CA-TPS blends were lower than the PLLA-PEG-PLLA/CA-free TPS blends for the same TPS content as shown in Figure 4. This indicates that the shorter CA-treated TPS chains showed more suppression of the crystallization of PLLA end-blocks in the blends than the longer CA-free TPS chains.

3.3 Thermal decomposition properties

The thermal decomposition properties of the blends were studied from thermogravimetric (TG) and derivative TG (DTG) curves as shown in Figures 5 and 6, respectively. The TG and DTG results including residue weight at 1,000°C, temperature at maximum decomposition rate of PLLA blocks (PLLA-$T_{d,max}$), and temperature at maximum decomposition rate of PEG blocks (PEG-$T_{d,max}$), are summarized in Table 2. The TG curve of pure PLLA-PEG-PLLA exhibited two weight loss steps in the ranges of 250–350°C and 350–450°C due to thermal decompositions of PLLA end-blocks and PEG middle-blocks, respectively (14–17). The pure PLLA-PEG-PLLA showed complete decomposition at a temperature around 450°C. From Table 2, the PLLA-$T_{d,max}$ and PEG-$T_{d,max}$ peaks of the pure PLLA-PEG-PLLA are seen to have been 294°C and 416°C, respectively.

From TG curves, it was found that all the blends also exhibited two weight loss steps in the ranges 100–380°C and 380–450°C. The temperature ranges for main thermal decompositions of PLLA end-blocks in the blends significantly shifted to higher temperature for both the blend series. From DTG curves, the PLLA-$T_{d,max}$ peaks of both the blend series dramatically shifted to higher temperature as the TPS content increased, indicating that the thermal stability of PLLA end-blocks in the blends increased with

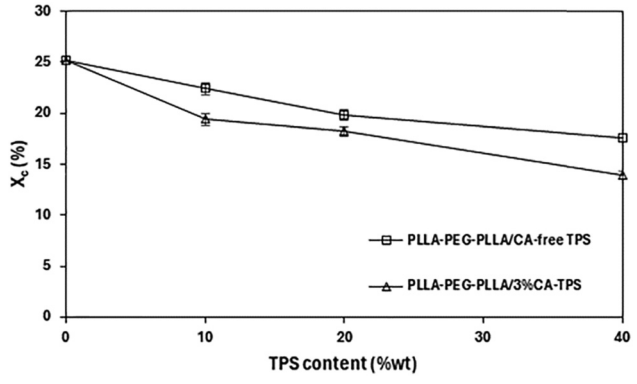

Figure 4: Effect of CA treatment on X_c of PLLA-PEG-PLLA/TPS blends.

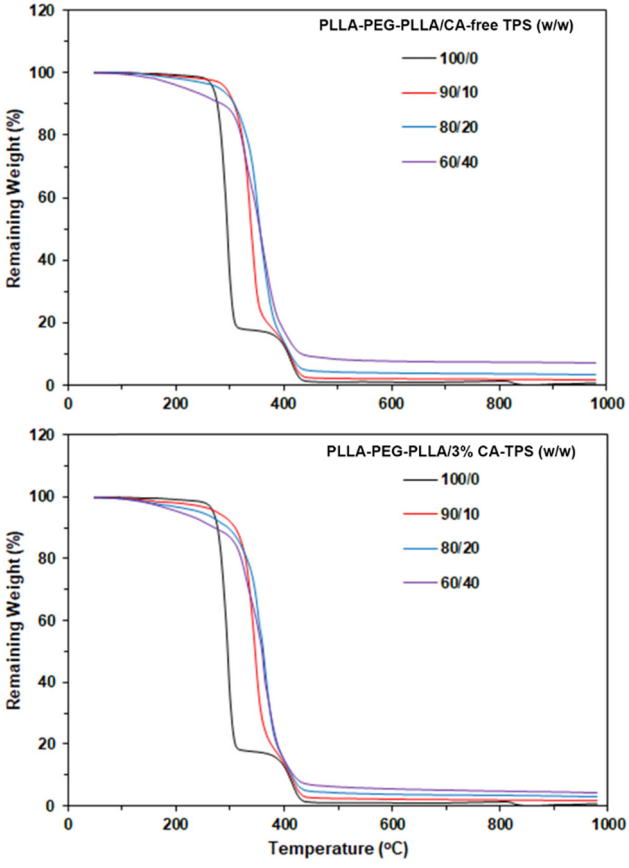

Figure 5: TG curves of (top) PLLA-PEG-PLLA/CA-free TPS and (bottom) PLLA-PEG-PLLA/3% CA-TPS blends for various blend ratios.

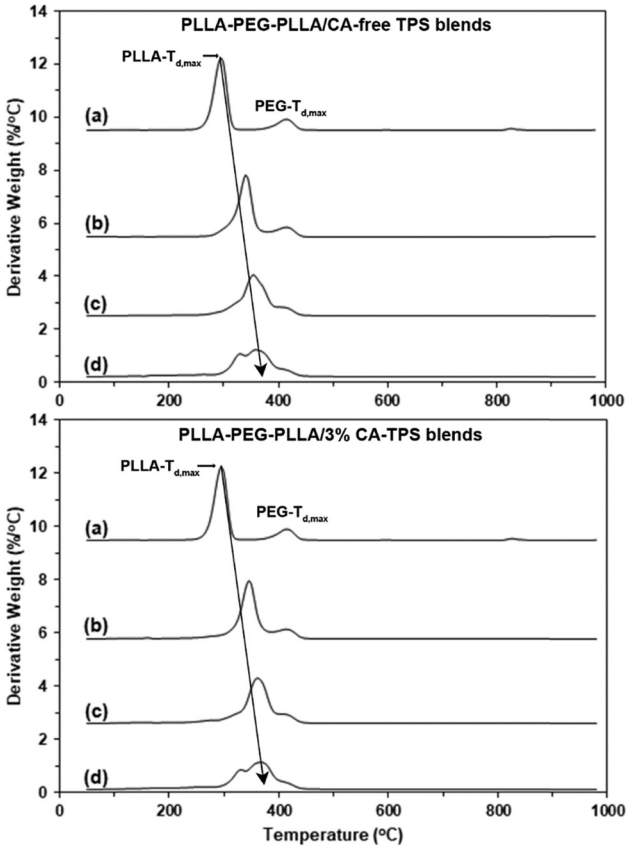

Figure 6: DTG curves of (top) PLLA-PEG-PLLA/CA-free TPS and (bottom) PLLA-PEG-PLLA/3% CA-TPS blends for various blend ratios ($T_{d,max}$ peaks as shown).

the increase in the TPS content. Hydrogen bonding could occur between the oxygen atoms of PEG middle-blocks and hydroxyl groups of starch to improve thermal stability of the PLLA end-blocks in PLLA-PEG-PLLA/starch blends (17). In addition, products from pyrolysis of starch induced a shielding effect that enhanced thermal stability of the compatible polymer/starch blends (17,19,30). However, the PEG-$T_{d,max}$ did not change significantly when the TPS was blended.

This indicates that the addition of TPS with and without CA treatment improved thermal stability of the PLLA end-blocks. However, the weight losses in the temperature range 100–300°C of the blends increased with the TPS content. This was due to lower thermal stability of the TPS than PLLA-PEG-PLLA (17,29). As would be expected, residue weight at 1,000°C of the blends increased as the TPS content increased because of increase in the TPS ashes.

From Table 2, it can be seen that the PLLA-$T_{d,max}$ peaks of PLLA-PEG-PLLA/3% CA-TPS blends were at higher temperature than the PLLA-PEG-PLLA/CA-free TPS blends for the same TPS content. This may be explained by the content of hydroxyl groups in 3% CA-TPS being more than the CA-free TPS as described in FTIR analysis reported above. Therefore, higher content of hydrogen bonds in the PLLA-PEG-PLLA/3% CA-TPS blends enhanced the higher thermal stability of the blends.

3.4 Phase morphology

The phase morphology of the blends was investigated from SEM images of the film cryo-fractured surfaces as shown in Figure 7. The cryo-fractured surface of pure PLLA-PEG-PLLA film in Figure 7(a) was homogeneous with rough surfaces suggesting it had a ductile character (13,14). All the blend films in Figure 7(b)–(g) showed that many voids which occurred from TPS phases fell out during film fractionation indicating phase separation between PLLA-PEG-PLLA matrices and dispersed TPS. The number and size of these voids increased as the TPS content increased.

It is clearly seen that the void sizes in the blends that contained 3% CA-TPS (Figure 7(e)–(g)) were smaller than in

Table 2: Thermal decomposition properties of PLLA-PEG-PLLA/TPS blends with and without CA treatment

PLLA-PEG-PLLA/TPS (w/w)	Residue weight at 1,000°C (%)[a]	PLLA-$T_{d,max}$ (°C)[b]	PEG-$T_{d,max}$ (°C)[b]
Pure PLLA-PEG-PLLA	0.3	294	416
PLLA-PEG-PLLA/CA-free TPS			
90/10	1.6	342	414
80/20	3.4	355	415
60/40	7.0	359	415
PLLA-PEG-PLLA/3% CA-TPS			
90/10	1.9	346	417
80/20	3.1	361	416
60/40	6.6	367	418

[a]Obtained from TG curves.
[b]Obtained from DTG curves.

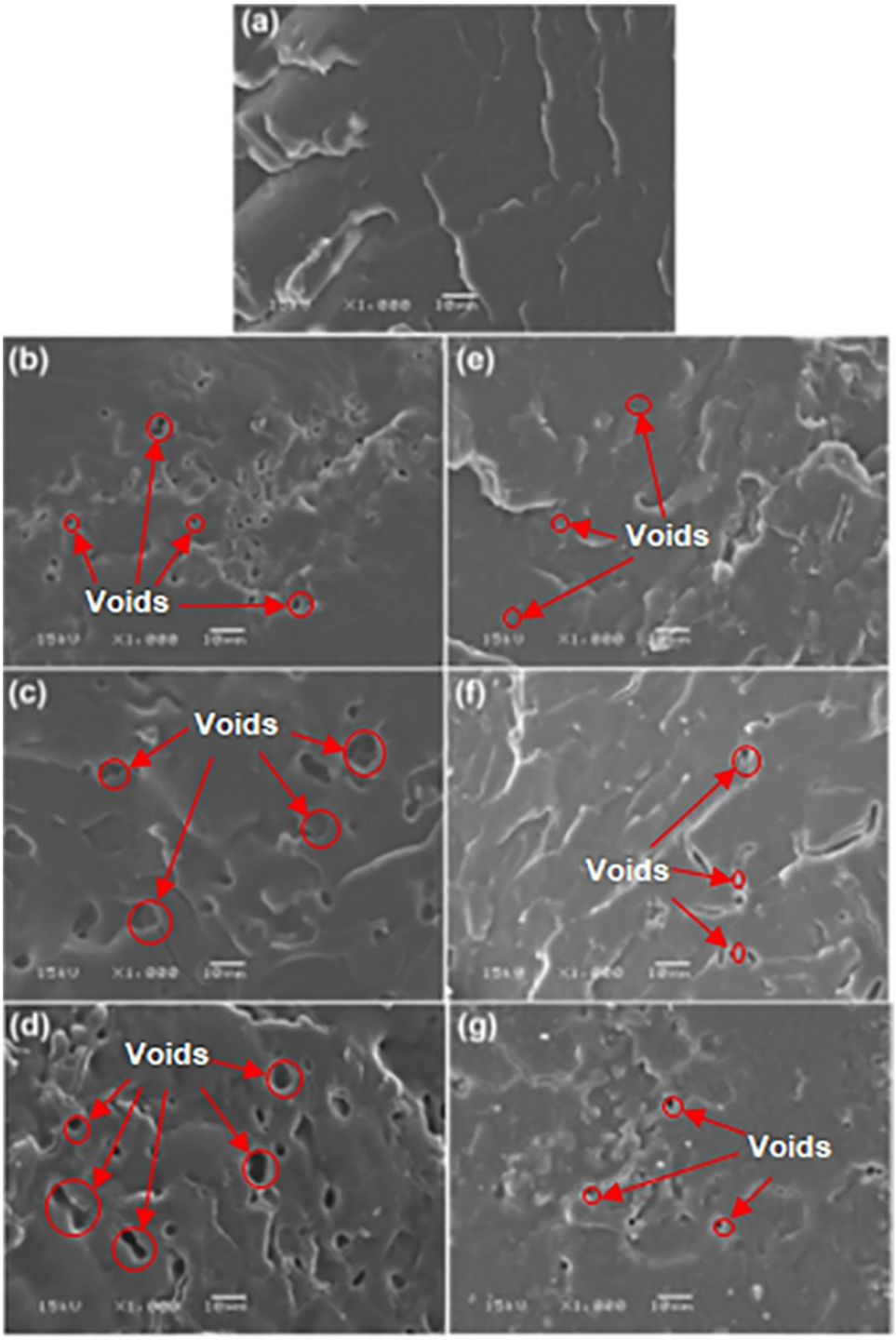

Figure 7: Cryo-fractured surfaces of (a) pure PLLA-PEG-PLLA and PLLA-PEG-PLLA/CA-free TPS blends for blend ratios of (b) 90/10, (c) 80/20, and (d) 60/40 (w/w) as well as PLLA-PEG-PLLA/3% CA-TPS blends for blend ratios of (e) 90/10, (f) 80/20, and (g) 60/40 (w/w) (all bar scales = 10 μm).

the blends containing CA-free TPS (Figure 7(b)–(d)) which suggested that the phase compatibility in the blends containing 3% CA-TPS was better than that in CA-free TPS (17,31,32). It has been reported that modification of TPS with CA improved the dispersion and phase compatibility of TPS in the polyethylene (33) and PLLA (24). This may be explained by acidic hydrolysis of starch with CA through melt processing leading to decreased molar mass of starch (23,28,34) and development of hydroxyl groups (23) to improve the phase compatibility between PLLA-PEG-PLLA and TPS. In addition, the unreacted CA could develop an *in situ* compatibilization effect by reacting with both the PLLA end-chains

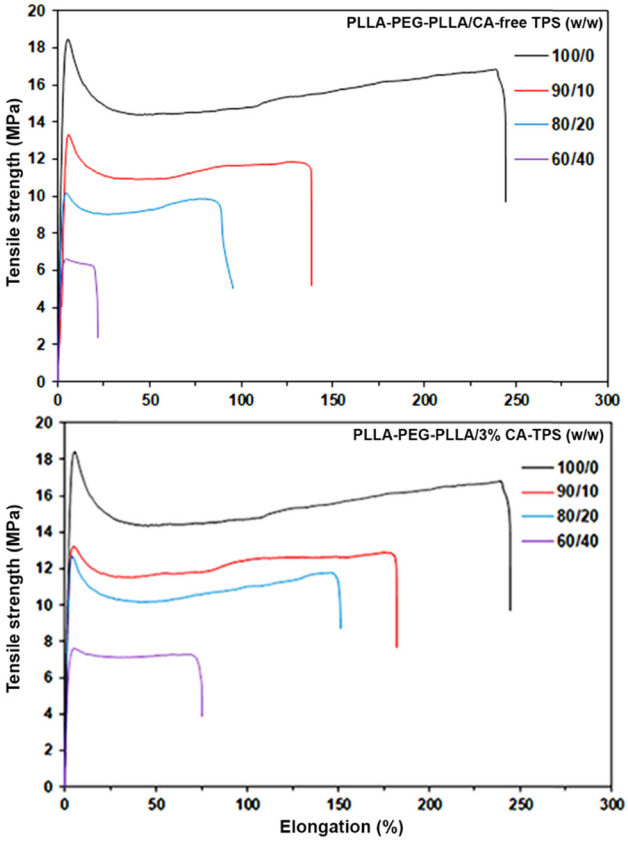

Figure 8: Tensile curves of (top) PLLA-PEG-PLLA/CA-free TPS and (bottom) PLLA-PEG-PLLA/3% CA-TPS blends for various blend ratios.

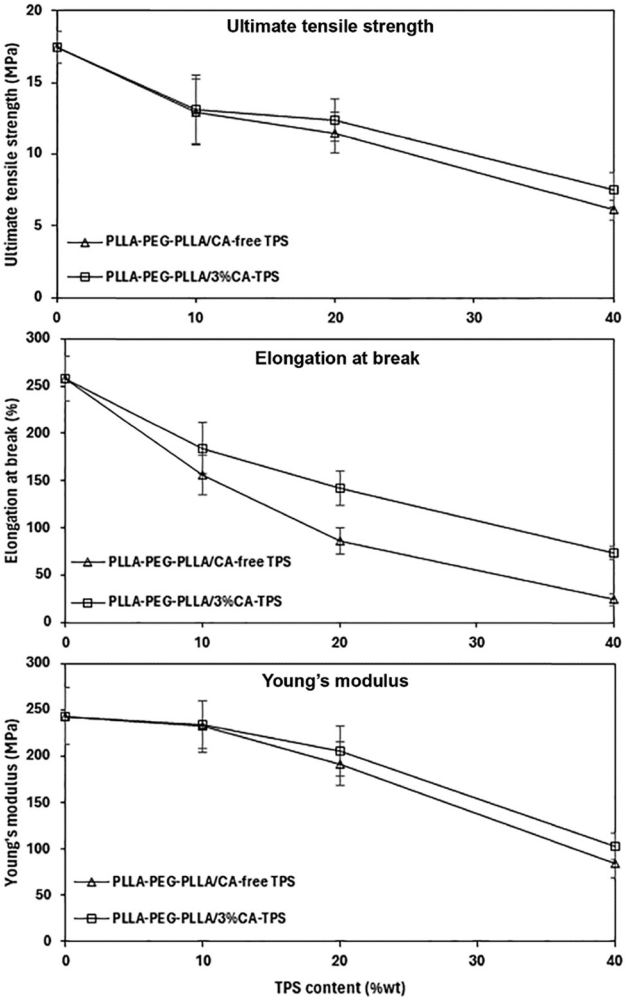

Figure 9: Effect of CA treatment on tensile properties of PLLA-PEG-PLLA/TPS blends.

and TPS during melt blending (35) and could create hydrogen bonding (36) to improve the interfacial interaction between PLLA and TPS.

3.5 Tensile properties

The tensile properties of the blend films were determined from stress–strain curves as shown in Figure 8 and the averaged tensile properties are summarized in Table 3. The ultimate tensile strength, elongation at break, and Young's modulus of the pure PLLA-PEG-PLLA films were 17.4 MPa, 258%, and 243 MPa, respectively. These tensile properties decreased when both the CA-free TPS and 3% CA-TPS were blended and the TPS content was increased.

Table 3: Tensile properties of PLLA-PEG-PLLA/TPS blends with and without CA treatment

Sample	Ultimate tensile strength (MPa)	Elongation at break (%)	Young's modulus (MPa)
Pure PLLA-PEG-PLLA	17.4 ± 1.1	258 ± 24	243 ± 31
PLLA-PEG-PLLA/CA-free TPS			
90/10	12.9 ± 2.3	156 ± 21	232 ± 28
80/20	11.5 ± 1.4	86 ± 14	192 ± 24
60/40	6.1 ± 0.7	24 ± 6	84 ± 15
PLLA-PEG-PLLA/3% CA-TPS			
90/10	13.1 ± 2.4	184 ± 27	234 ± 26
80/20	12.4 ± 1.5	142 ± 18	205 ± 27
60/40	7.5 ± 1.2	73 ± 7	103 ± 14

This is due to the poor mechanical properties of the TPS (12,19,20). However, the tensile properties of the blend films containing 3% CA-TPS were higher than the blend films that contained CA-free TPS for the same TPS content as shown in Figure 9. This may be due to the good phase compatibility in the blend films that contained 3% CA-TPS as described above in the SEM analysis. The CA treatment can increase the tensile properties of the PLLA/TPS blends by improving its phase compatibility (24). The tensile results support a conclusion that the tensile properties of the PLLA-PEG-PLLA/TPS blends were improved by CA treatment of TPS.

4 Conclusion

In this study, TPS was treated with 3 wt% CA (3% CA) before melt blending with the PLLA-PEG-PLLA for PLLA-PEG-PLLA/TPS blend ratios of 90/10, 80/20, and 60/40 (w/w). The FTIR analysis indicated that both the acetylation and acidic hydrolysis reactions of TPS with CA had occurred. For PLLA-PEG-PLLA/TPS blends, the crystallization ability of PLLA-PEG-PLLA matrices decreased and the thermal stability increased as the TPS content increased, as determined from DSC and TGA analyses, respectively. The addition of 3% CA-TPS showed more suppression in crystallization of the PLLA end-blocks and more improvement in thermal stability of the PLLA end-blocks for the PLLA-PEG-PLLA/TPS blends than with the addition of CA-free TPS. The blends containing 3% CA-TPS showed better phase compatibility and higher tensile properties than those of the blends containing CA-free TPS for same blend ratio as investigated from SEM analysis and tensile test, respectively. PLLA-PEG-PLLA/TPS treated with CA blends can be used as fully biodegradable and flexible bioplastics.

Acknowledgements: The authors like to thank the Centre of Excellence for Innovation in Chemistry (PERCH-CIC), Office of the Higher Education Commission, Ministry of Education, Thailand for providing the tensile test.

Funding information: This research project is financially supported by Thailand Science Research and Innovation (TSRI).

Author contributions: Yaowalak Srisuwan: conceptualization, methodology, investigation, writing – original draft, and funding acquisition; Prasong Srihanam: validation, investigation, writing – review and editing; Theeraphol Phromsopha: validation, investigation, and writing – review and editing; Yodthong Baimark: conceptualization, methodology, investigation, writing – original draft, writing – review and editing, supervision, project administration, and funding acquisition.

Conflict of interest: The authors have no conflict of interest.

References

(1) Silva D, Kaduri M, Poley M, Adir O, Krinsky N, Shainsky-Rotiman J, et al. Biocompatibility, biodegradation and excretion of polylactic acid (PLA) in medical implants and theranostic systems. Chem Eng J. 2018;340:9–14.

(2) Mishra RK, Ha SK, Verma K, Tiwari SK. Recent progress in selected bio-nanomaterials and their engineering applications: An overview. J Sci: Adv Mater Dev. 2018;3:263–88.

(3) Standau T, Castellón SM, Delavoie A, Christian Bonten C, Altstädt V. Effects of chemical modifications on the rheological and the expansion behavior of polylactide (PLA) in foam extrusion. e-Polymers. 2019;19:297–304.

(4) Donate R, Monzón M, Alemán-Domínguez ME. Additive manufacturing of PLA-based scaffolds intended for bone regeneration and strategies to improve their biological properties. e-Polymers. 2020;20:571–99.

(5) Huang D, Hu Z-D, Liu T-Y, Lu B, Zhen Z-C, Wang G-X, et al. Seawater degradation of PLA accelerated by water-soluble PVA. e-Polymers. 2020;20:759–72.

(6) Albuquerque RQ, Brütting C, Tobias Standau T, Ruckdäschel H. A machine learning investigation of low-density polylactide batch foams. e-Polymers. 2022;22:318–31.

(7) Kumari SVG, Pakshirajan K, Pugazhenthi G. Recent advances and future prospects of cellulose, starch, chitosan, polylactic acid and polyhydroxyalkanoates for sustainable food packaging applications. Int J Biol Macromol. 2022;221:163–82.

(8) Jin FL, Hu RR, Park SJ. Improvement of thermal behaviors of biodegradable poly(lactic acid) polymer: a review. Compos B. 2019;164:287–96.

(9) Song Q. Thermal and mechanical properties of poly(lactic acid)/poly(butylene adipate-co-terephthalate)/calcium carbonate composite with single continuous morphology. e-Polymers. 2022;22:1007–20.

(10) Fu X, Zhang T, Zhang W, Zhong Y, Fang S, Wang G, et al. Melt-blended PLA/curcumin-cross-linked polyurethane film for enhanced UV-shielding ability. e-Polymers. 2023;23:20230009.

(11) Akrami M, Ghasemi I, Azizi H, Karrabi M. A new approach in compatibilization of the poly(lactic acid)/thermoplastic starch (PLA/TPS) blends. Carbohyd Polym. 2016;144:254–62.

(12) Chotiprayon P, Chaisawad B, Yoksan R. Thermoplastic cassava starch/poly(lactic acid) blend reinforced with coir fibres. Int J Biol Macromol. 2020;156:960–8.

(13) Yun X, Li X, Jin Y, Sun W, Dong T. Fast crystallization and toughening of poly(L-lactic acid) by incorporating with poly(ethylene glycol) as a middle block chain. Polym Sci Ser A. 2018;60:141–55.

(14) Baimark Y, Rungseesantivanon W, Prakymoramas N. Improvement in melt flow property and flexibility of poly(L-Lactide)-*b*-poly(ethylene glycol)-*b*-poly(L-Lactide) by chain extension reaction for potential use as flexible bioplastics. Mater Des. 2018;154:73–80.

(15) Baimark Y, Srisuwan Y. Thermal and mechanical properties of highly flexible poly(L-Lactide)-*b*-poly(ethylene glycol)-*b*-poly(L-Lactide) bioplastics: effects of poly(ethylene glycol) block length and chain extender. J Elastom Plast. 2020;52(2):142–58.
(16) Baimark Y, Rungseesantivanon W, Prakymoramas N. Synthesis of flexible poly(L-lactide)-*b*-polyethylene glycol-*b*-poly(L-lactide) bioplastics by ring-opening polymerization in the presence of chain extender. e-Polymers. 2020;20(1):423–29.
(17) Srisuwan Y, Baimark Y. Thermal, morphological and mechanical properties of flexible poly(L-lactide)-*b*-polyethylene glycol-*b*-poly(L-lactide)/thermoplastic starch blends. Carbohyd Polym. 2022;283:119155.
(18) Thongsomboon W, Srihanam P, Baimark Y. Preparation of flexible poly(l-lactide)-*b*-poly(ethylene glycol)-*b*-poly(l-lactide)/talcum/thermoplastic starch ternary composites for use as heat-resistant and single-use bioplastics. Int J Biol Macromol. 2023;230:123172.
(19) Sessini V, Arrieta MP, Raquez J-M, Dubois P, Kenny JM, Peponi L. Thermal and composting degradation of EVA/Thermoplastic starch blends and their nanocomposites. Polym Degrad Stab. 2019;159:184–98.
(20) Zaaba NF, Ismail H. A review on tensile and morphological properties of poly(lactic acid) (PLA)/thermoplastic starch (TPS) blends. Polym-Plast Tech Mat. 2019;58:1945–64.
(21) Wang N, Yu J, Chang PR, Ma X. Influence of citric acid on the properties of glycerol-plasticized dry starch (DTPS) and DTPS/poly (lactic acid) blends. Polym Comps. 2007;59(9):409–17.
(22) Wang N, Yu J, Ma X. Preparation and characterization of compatible thermoplastic dry starch/poly(lactic acid). Starke. 2008;29(5):551–9.
(23) Kahar AWM, Ismail H, Othman N. Morphology and tensile properties of high-density polyethylene/natural rubber/thermoplastic tapioca starch blends: The effect of citric acid-modified tapioca starch. J Appl Polym Sci. 2012;125:768–75.
(24) Ibrahim N, Wahab MKA, Uylan DN, Ismail H. Physical and degradation properties of polylactic acid and thermoplastic starch blends – effect of citric acid treatment on starch structures. Bioresour. 2017;12(2):3076–87.
(25) Liu W, Wu X, Ou Y, Liu H, Zhang C. Electrically conductive and lightweight branched polylactic acid-based carbon nanotube foams. e-Polymers. 2021;21:96–107.
(26) Cuevas-Carballo ZB, Duarte-Aranda S, Canch´ e-Escamilla G. Properties and biodegradation of thermoplastic starch obtained from grafted starches with poly(lactic acid). J Polym Environ. 2019;27:2607–17.
(27) Reddy N, Yang Y. Citric acid cross-linking of starch films. Food Chem. 2010;118(3):702–11.
(28) Carvalho AJF, Zambon MD, Curvelo AA, Gandini A. Thermoplastic starch modification during melt processing: Hydrolysis catalyzed by carboxylic acids. Carbohyd Polym. 2005;62(4):387–90.
(29) Ferri JM, Garcia-Garcia D, Carbonell-Verdu A, Fenollar O, Balart R. Poly(lactic acid) formulations with improved toughness by physical blending with thermoplastic starch. J Appl Polym Sci. 2017;134:45751.
(30) Nguyen DM, Vu TT, Grillet A-C, Ha Thuc H, Ha, Thuc CN. Effect of organoclay on morphology and properties of linear low density polyethylene and Vietnamese cassava starch biobased blend. Carbohyd Polym. 2016;2016(136):163–70.
(31) Wootthikanokkhan J, Kasemwananimit P, Sombatsompop N, Kositchaiyong A, Isarankura, na Ayutthaya S, Kaabbuathong N. Preparation of modified starch-grafted poly(lactic acid) and a study on compatibilizing efficacy of the copolymers in poly(lactic acid)/thermoplastic starch blends. J Appl Polym Sci. 2012;126:388–95.
(32) Noivoil N, Yoksan R. Oligo(lactic acid)-grafted starch: A compatibilizer for poly(lactic acid)/thermoplastic starch blend. Int J Biol Macromol. 2020;160:506–17.
(33) Wang N, Yu JG, Ma XF, Han CM. High performance modified thermoplastic starch/linear low-density polyethylene blends in one-step extrusion. Polym Compos. 2007;28(1):89–97.
(34) Da Róz AL, Zambon MD, Curvelo AAS, Carvalho AJF. Thermoplastic starch modified during melt processing with organic acids: The effect of molar mass on thermal and mechanical properties. Ind Crops Prod. 2011;33(1):152–7.
(35) Murillo EA. *In situ* compatibilization of thermoplastic starch/polylactic acid blends using citric acid. Macromol Res. 2023;31(2):157–69.
(36) Chabrat E, Abdillahi H, Rouilly A, Rigal L. Influence of citric acid and water on thermoplastic wheat flour/poly(lactic acid) blends. I: Thermal, mechanical and morphological properties. Ind Crops Prod. 2012;37(1):238–46.